Dynamics of the sputtering of water from ice films by collisions with energetic xenon atoms

Daniel R. Killelea, K. D. Gibson, Hanqiu Yuan, James S. Becker, and S. J. Sibener

Citation: The Journal of Chemical Physics **136**, 144705 (2012); doi: 10.1063/1.3699041
View online: http://dx.doi.org/10.1063/1.3699041
View Table of Contents: http://scitation.aip.org/content/aip/journal/jcp/136/14?ver=pdfcov
Published by the AIP Publishing

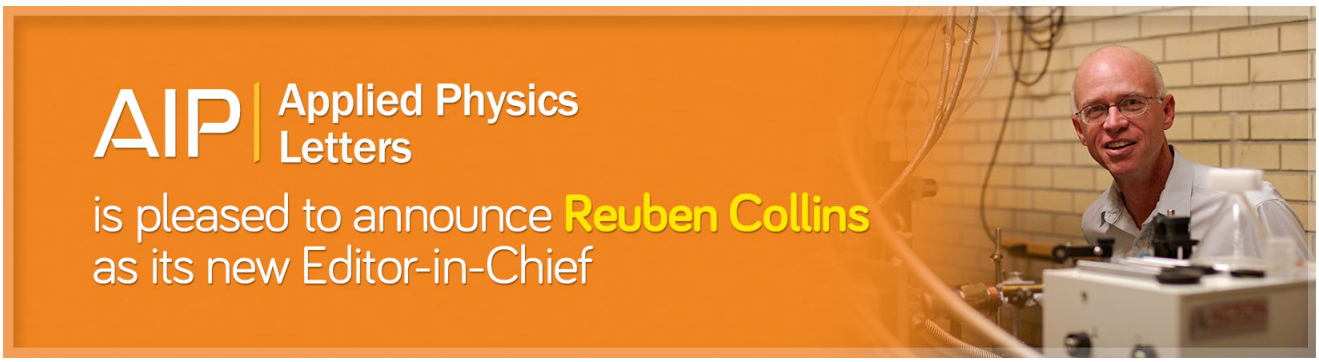

Dynamics of the sputtering of water from ice films by collisions with energetic xenon atoms

Daniel R. Killelea,[a] K. D. Gibson, Hanqiu Yuan, James S. Becker,[b] and S. J. Sibener[c]
The James Franck Institute and Department of Chemistry, The University of Chicago, 929 E. 57th Street, Chicago, Illinois 60637, USA

(Received 11 February 2012; accepted 14 March 2012; published online 11 April 2012)

The flow of energy from the impact site of a heavy, translationally energetic xenon atom on an ice surface leads to several non-equilibrium events. The central focus of this paper is on the collision-induced desorption (sputtering) of water molecules into the gas-phase from the ice surface. Sputtering is strongly activated with respect to xenon translational energy, and a threshold for desorption was observed. To best understand these results, we discuss our findings in the context of other sputtering studies of molecular solids. The sputtering yield is quite small; differential measurements of the energy of xenon scattered from ice surfaces show that the ice efficiently accommodates the collisional energy. These results are important as they quantitatively elucidate the dynamics of such sputtering events, with implications for energetic non-equilibrium processes at interfaces. © *2012 American Institute of Physics*. [http://dx.doi.org/10.1063/1.3699041]

INTRODUCTION

Energetic collisions between gas-phase atoms or molecules and ice surfaces are nearly ubiquitous in nature. Given the disparity between the temperature of the substrate and that of the incident species, these collisions occur under non-equilibrium conditions. The collision-induced desorption (CID), or sputtering, of molecules from surfaces is of fundamental interest to understanding the chemical behavior of adsorbed molecules on surfaces, and is an important method for preparing novel materials.[1,2] Sputtering is widely employed for surface preparation,[3] depth profiling of materials,[4] preparation of special surface structures to study strain effects for surface reactivity,[5] and fabrication of nanostructures.[6,7] Moreover, such CID processes are inherent to all studies of surface chemistry that involve highly translationally energetic events that alter the surface coverage and composition of reactive overlayers. Ion beams are often used because they are readily prepared in vacuum, their focusing and alignment is well established, and they can achieve very high energies (up to several MeV) for the sputtering of strongly bound systems. However, the combination of highly reactive ions and high collision energies often leads to significant undesired physical damage and chemical changes to more weakly bound systems, such as molecular solids or arrays of nanostructures.[3,8]

When energetic atoms collide with a metal surface decorated with adsorbed small molecules (total coverage up to a few layers), the energy from the impact of the incident atom with the surface adsorbate can lead to one of several possible outcomes. The impact may cause dissociation of the molecule adsorbed to the surface.[1] In the case of the bombardment of hydrogen atoms on a metal surface with energetic, heavy atoms, collision-induced absorption has been established where the impact drives surface-bound H atoms into the bulk of the metal.[9] Additionally, the impact may induce diffusion or desorption of adsorbates on the surface.[10] Finally, collision-induced recombinative desorption occurs when the impact imparts sufficient energy for an adsorbed atom to diffuse across the surface and react with another adsorbed atom to form a molecule that promptly desorbs.[11] The relative importance of each of these outcomes depends on several factors, including the incident energy of the energetic atom, the strength of the surface-adsorbate bond, and the mobility of the molecules on the surface. Collision-induced desorption is favorable at the high collision energies typical of ion sputtering, as demonstrated by studies of the bombardment of ice surfaces with energetic ions.[2,12–14] However, in addition to desorption, these highly energetic and reactive ions may also cause dissociation of surface molecules, leading to significant chemical alteration and extensive surface damage.[15] There are fewer reported instances where the sputtering or surface treatment of ices using gentler, neutral, projectiles has been explored.[15–19] It would be highly advantageous to selectively remove molecules from a surface without unwanted side effects. For example, in the fabrication of nanoarrays, loosely bound, unwanted, materials remaining on the surface could be removed by neutral bombardment, with minimal disruption of the desired nanostructures.

Molecular solids, such as ice, have low cohesion energies, typically less than 1 eV (where eV implies eV per molecule or atom) when compared to solids held together by covalent, metallic, or ionic bonds.[12,20,21] Molecular solids are bound by comparatively weak van der Waals forces or in the case of water ice, stronger hydrogen bonds. Because of their lower cohesive strength, sputtering is energetically accessible by beams of neutral atoms. As mentioned, avoiding the use

[a]Present address: Department of Chemistry, Loyola University Chicago, 1068 W. Sheridan Ave., Chicago, Illinois 60660, USA.
[b]Present address: Intel Corporation, Hillsboro, Oregon 97124, USA.
[c]Author to whom correspondence should be addressed. Electronic mail: s-sibener@uchicago.edu.

of high-energy ion sources and instead sputtering with gentler, neutral species offers a "soft" method for surface treatments of molecular solids. Collisional energy readily facilitates desorption in systems where heavy projectiles strike a light molecule bound to a surface of heavier atoms; momentum (energy) exchange between the adsorbate and the heavier surface atoms is inefficient due to the mass mismatches of the system and accumulates in the adsorbate–surface bond, leading to desorption or even reaction of the adsorbed molecules.[1,9,22,23] Because the masses of molecules on both the surface and in the bulk of the solid are the same, momentum transferred by a projectile to the surface molecules is readily dispersed through the solid matrix, akin to a "Newton's Cradle." Furthermore, collision energy may be dissipated through distortions of the relatively malleable lattice of molecular solids. Finally, accommodation of the collision energy in molecular solids may also be facilitated by excitation of internal states of both surface and bulk molecules.[10] The net result of the presence of these quenching channels is the efficient dissipation of the collision energy from the incident projectile; this leaves little energy to desorb molecules from the surface. Sputtering of water from ice has been reported using protons,[24,25] Xe^+,[26] He^+ and O^+,[27] and Ar^+[12] with energies in the keV range, but sputtering with low (below 1 keV) energy neutrals has not been thoroughly examined.

Water desorption is also possible when ice is exposed to ultraviolet light. Vacuum ultraviolet light, $\lambda < 200$ nm, photodissociates H_2O into H atoms and OH radicals. The H atoms are translationally excited, and their collisions with surface water molecules can lead to desorption. It is important to note that this photochemical sputtering is enhanced by light-induced changes to the hydrogen bond network resulting in repulsive interactions between the photoproducts and water molecules.[28,29] In a similar fashion, protons impinging on an ice surface interact strongly with the water molecules, disrupt the hydrogen bonding network, cause restructuring of the ice, and this rearrangement leads to ejection of a surface water molecule. Calculations predict sputtering yields of 10%–20% for exposure of crystalline ice to 0.1 to 4 eV protons, with no dependence on the incident angle of the protons.[24,25]

This paper presents results from of a study where ice surfaces were sputtered by comparatively low incident energy (<7 eV) xenon atoms and show that, despite the ability of the surface to absorb energy, collision-induced desorption of water occurs when ice surfaces were bombarded with energetic xenon atoms. The sputter yields and CID cross sections for desorption of water from both H_2O and D_2O ices were determined, as well as the energy of the scattered xenon to better understand how collisional energy was exchanged. These results show that the incident xenon atoms lost most of their initial energy to the ice and that the scattering process was more complex than a single bimolecular collision event that can be described using a simple hard-cube model. Despite efficient accommodation of the incident energy of the xenon atoms, sufficient energy is available to overcome the rather strong hydrogen bonding of the ice and expel a small but significant number of water molecules from the ice surface. The sputtering process shows an energetic threshold that coincides with the enthalpy of sublimation and the dissociation energy of small water clusters, whereupon energy transfer from the projectile is able to overcome the cohesive forces of the ice and liberate water molecules from the solid phase to the gas phase.

EXPERIMENTAL DETAILS

Two complementary sets of experiments were performed to study the dynamics of the interaction of energetic xenon atoms with ice surfaces. Of particular interest were the sputter yield and energy of the scattered xenon. The first set of experiments measured the sputter yield by using Fourier-transform infrared reflection-absorption spectroscopy (IRRAS) to measure the change in ice films deposited on an Au(111) substrate. In the second set of experiments, a differentially pumped, rotatable quadrupole mass spectrometer (QMS) detected the scattered xenon atoms. Details of the two instruments have been provided in previous publications, so only brief descriptions are provided here.[30,31]

The IRRAS data were collected using a Nicolet 6700 FTIR spectrometer with a liquid nitrogen cooled MCT/A detector. The p-polarized light from the spectrometer was directed onto the Au(111) sample at a 75° incidence through a series of optics enclosed in a dry-N_2 purged box. Each IRRAS spectrum is an average of 25 scans with a resolution of 4 cm^{-1}. The Au(111) sample was housed in an ultra-high vacuum (UHV) chamber and mounted on a precision manipulator for accurate placement of the sample. Au surface cleanliness was verified with Auger electron spectroscopy and surface order was checked using low-energy electron diffraction. The mount for the Au(111) crystal was cooled with liquid nitrogen and the temperature was controlled (115 to 1300 K) using a combination of radiative and electron bombardment heating. The temperature was measured using a type-K thermocouple affixed between the crystal and the sample mount and a proportional integral differential feedback loop controller (Eurotherm) was used to set the sample temperature. Ice films were grown on the gold substrate by dosing with a molecular beam of water. The beam was formed by bubbling helium through a reservoir of either H_2O or D_2O. The incident flux of water in the beam was about 0.1 layer s^{-1}. For the data presented here, the ice films were between 50 and 200 layers thick. Molecular beam deposition is well controlled and limits the amount of water introduced to the UHV chamber, thus minimizing any unwanted background deposition of water onto the ice surface under study during subsequent experiments. The morphology (crystalline vs. amorphous) of the ice film grown on the Au(111) substrate was determined by the temperature of the substrate. Above 150 K, the film was polycrystalline ice, with a stochastic arrangement of the crystallites, and deposition of water at 120 K resulted in the growth of a glassy, metastable form of ice, known as amorphous solid water (ASW).[21,32] After the ice film was grown to the desired thickness, the ice was exposed to a beam of xenon atoms and the sputtering rate was determined from the change in the integrated IR intensity of either the O–H (2800 to 3800 cm^{-1}) or O–D (2200 to 2800 cm^{-1}) stretch regions. The incident translational energy (E_I) of xenon in the beam was between 2 and 6.5 eV with a width ($\Delta E/E_I$) less then 0.15

and was selected by varying the temperature of the beam nozzle (300–700 K) and seeding the xenon (1%) in either helium or hydrogen. The speed of the xenon atoms in the beam was measured with time-of-flight techniques and their average energy was calculated from a shifted Boltzmann distribution fitting procedure.[33] For most experiments, the xenon atoms impinged at normal incidence. As long as the ice thickness was greater than 20 layers, the decrease in integrated intensity of the water stretch peak was linear with respect to xenon exposure for both H_2O and D_2O ices for all incident energies of the xenon atoms. Water does not wet the gold surface and forms three-dimensional ice islands instead of planar sheets; the results of this is that the desorption kinetics and surface area are inhomogeneous until the islands grow together, between 30 and 50 layers of ice coverage.[30,34,35] To avoid any thickness dependency on the sputtering rate, films of around 100 layers coverage were used.

In order to quantify the IRRAS data, a conversion factor is needed to convert the measured integrated absorbance into layers of ice on the Au(111) substrate is needed. The factor η was determined by backfilling the UHV chamber to 1×10^{-7} Torr H_2O or D_2O, and taking IRRAS measurements as the water vapor condensed onto the surface. For these experiments, the Au(111) crystal was held at 120 K, where the sticking coefficient was essentially unity,[30] and where desorption is negligible compared to uptake, so the 1×10^{-7} Torr pressure leads to an accumulation of 0.1 layers s^{-1} on the Au(111) crystal. Deposition at this low temperature results in an ASW film, so the sample was warmed after deposition to crystallize the ice and thus obtain the conversion factors for crystalline ice. Backfilling at 145 K to deposit crystalline ice gave indistinguishable results versus growing amorphous solid water and crystallizing it. The spectra of the ices grown by beam deposition and background dosing are similar, and the conversion factors were found to be 5.92 and 2.39 layers per integrated absorbance unit for H_2O and D_2O, respectively. If the shape of the absorption features changed either during deposition or during xenon exposure, these conversion factors would no longer be accurate. However, any observed changes in the absorption features for the ice on the gold surface were minor and had little effect on the results.

The scattering experiments were conducted in a separate UHV chamber with three molecular beam lines each coincident on a Rh(111) single crystal. A doubly differentially pumped, rotatable QMS measured the energy of the scattered xenon atoms. Ice films were grown on the Rh(111) single crystal; as discussed in previous publications,[15,30,36] the morphology of ice grown on Rh(111) is highly dependent on the initial oxygen coverage and deposition temperature. To form a polycrystalline ice surface similar to those used in the IRRAS experiments, very thick ice films where any structure imparted by the Rh(111) substrate vanishes were used for these scattering studies. To grow these films, 0.5 monolayers of oxygen were first deposited on the Rh(111). Films of nearly 1000 layers D_2O were then deposited from a molecular beam of D_2O/He. The D_2O background in the detector is significantly less than the H_2O background, so D_2O ices were used in an attempt to detect the sputtered water. Unlike a previous study of the sputtering of water from ultra-thin films of ice on Rh(111) using a high-intensity pulsed Ar source,[15] the signal-to-noise ratio in the detector was too small to detect any ablated water because of the low sputtering rate of the continuous xenon beam.

RESULTS AND DISCUSSION

Crystalline ice films of between 50 and 200 layers thick were grown on an Au(111) substrate at 150 K. Once deposited, the ice was cooled to 125 K and exposed to a continuous beam of seeded xenon atoms with incident energies between 2.0 and 6.5 eV. Figure 1 shows the representative IR spectra of D_2O during their deposition from the molecular beam on Au(111) at 150 K. The spectra at several thicknesses of the ice are shown in Figure 1(a), and the scaled spectra are shown in Figure 1(b). The spectra had the baseline subtracted, and their absorbance maxima set to 1. Plotting in this manner highlights subtle changes in the absorption features that are typically obscured by the large changes in intensity as the film thickens. As shown by the figure, there are only minor changes in the shape of the absorption features as the film thickens to 180 layers. The O–D or O–H stretch peak was integrated to quantify the film thickness, and plot of the peak integral vs. dose time is shown in Figure 1(c). The slight change in the absorption peak shape did not affect the linear relationship between the integrated absorption and film thickness in the thickness regime used here. Finally, as mentioned in a previous publication,[30] the vacuum–ice interface area is proportional to the intensity of the dangling O–D (or O–H) bond near 2725 cm^{-1}. An expansion of the dangling bond portion of the spectrum is shown in Figure 1(d). From the plot it is apparent, even at 10 ice layers of ice, that the ice–vacuum interface has reached a steady-state surface area.

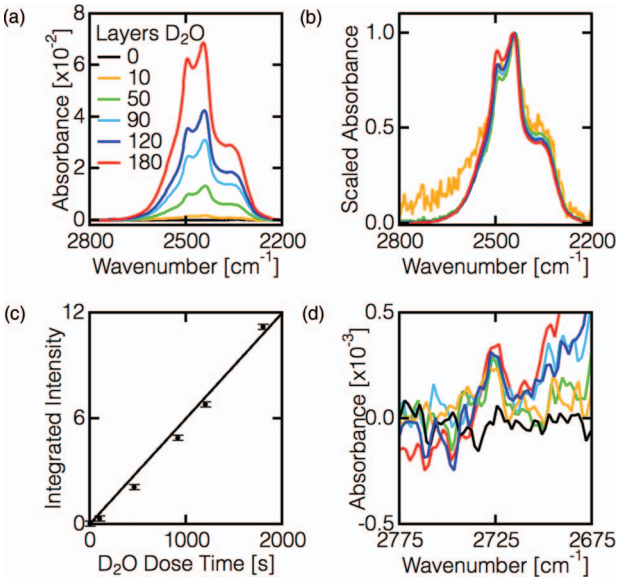

FIG. 1. Infrared spectra of crystalline D_2O ice on Au(111) at 150 K during water deposition. The absorbance and scaled absorbance of the ice film at six different thicknesses is shown in panels (a) and (b), respectively. In panel (c), the linear relationship between film thickness and the integral of the O–D stretch peak is shown. Panel (d) zooms in on the dangling O–D peak at 2725 cm^{-1} from panel (a). This peak is a measure of the surface area of the ice, and saturates near 10 layers of D_2O (yellow line).

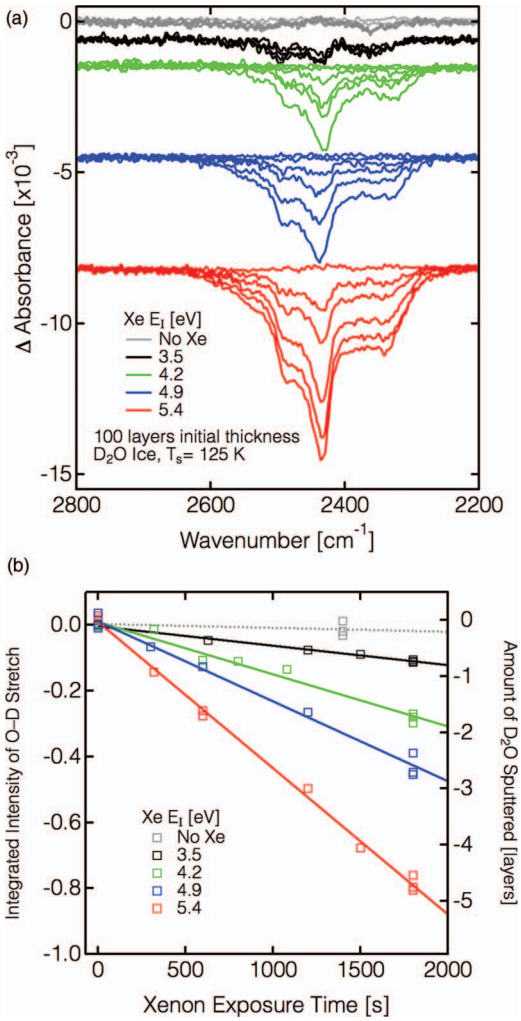

FIG. 2. Collision-induced desorption of water from ice surfaces. Spectra were taken every 5 min during xenon exposure and the change in the O–D stretch absorption feature is shown in panel (a). Crystalline D_2O ice films on Au(111) with an initial thickness of 100 layers were exposed to xenon atoms with average $E_I = 3.5$ eV (black), 4.2 eV (green), 4.9 eV (blue), and 5.4 eV (red) at $T_s = 125$ K. Each E_I group of spectra is offset for clarity and is referenced to spectra taken before exposure. Also shown are the absorption changes when ice was exposed to a beam of H_2 atoms (grey) as a control. The sputter rate is the slope of the lines on the plot of the integrated intensity change of the O–D stretch as a function of xenon exposure time in panel (b). The total amount of water desorbed from the film is given by the left-hand axis.

Once the ice film was deposited and characterized, it was exposed to a beam of translationally energetic xenon atoms. Under all conditions studied here, energetic xenon atoms made the ice films thinner by causing desorption of water molecules from the ice surface. IRRAS spectra were taken *in situ* to quantify any changes in the spectra indicating mass loss or even changes in the morphology. Figure 2(a) shows the IRRAS spectra taken during exposure of a crystalline ice film at 125 K to xenon atoms at several incident kinetic energies. The data are plotted as the change in absorption, rather than the absorption spectra. Each spectrum was referenced to the absorbance of the ice film before exposure to xenon. As presented, negative peaks indicate loss, while positive peaks indicate gain. If the absorption features were shifting, derivative-shaped peaks would be observed. No positive peaks were observed in the spectra under any xenon dose conditions, but rather, only negative peaks were found, indicating xenon exposure causes the ice to lose material via sputtering.

The ice loss was quantified by plotting the change in the integrated intensity of the O–D or O–H stretch peak as the xenon dose proceeds. These data are plotted in Figure 2(b) for four different xenon incident energies incident on crystalline D_2O. Under all xenon dose conditions used here, the change in O–D or O–H optical absorption strength is linear with respect to the length of the xenon exposure. In addition, the grey data points and dotted line show the change in the O–D or O–H stretch peak with the xenon beam blocked. There is still a slight loss in intensity, -1.2×10^{-5} Integrated Abs s^{-1}, which corresponds to a loss of near 7×10^{-5} layers D_2O s^{-1}. This is very close to the desorption rate calculated from the values reported by Speedy *et al.* for D_2O desorbing from D_2O ice at 127.5 K.[21] This serves as a convenient calibration for the temperature measurement, and establishes the observed decrease in IRRAS intensity as being caused solely by action of the incident xenon atoms. Sputtering of water from ice was the result of collisions with incident xenon alone; a beam of pure H_2 did not cause any sputtering.

The deposited ice films were exposed to xenon atoms having several incident kinetic energies, and the amount of water sputtered from the ice was quantified with IRRAS. The change in ice coverage with respect to time is the product of the collision-induced desorption cross section, $\sigma_{\mathrm{CID}}(E_I)$, the incident xenon flux, $\Phi_{\mathrm{Xe}} = 2.7 \times 10^{14}$ Xe cm^{-2} s^{-1}, and θ^0_{ice}, the number density of surface water molecules, 1.06×10^{15} water molecules cm^{-2},[21] shown in Eq. (1):

$$-\frac{d\theta_{\mathrm{ice}}}{dt} = \sigma_{\mathrm{CID}}(E_I)\,\Phi_{\mathrm{Xe}}\theta^0_{\mathrm{ice}}. \tag{1}$$

As shown in Figure 2, the IRRAS spectra decreased monotonically and retained the shape of the CI spectrum. The homogenous change in the IRRAS spectra is indicative of the sputtering process being randomly distributed across the surface, with no alteration of the phase or morphology of the ice as to effect sputtering, and there were no areas of preferential sputtering for the ice thicknesses used in these experiments. Thus, number density of water molecules at the surface, θ^0_{ice}, is effectively a constant. The observed sputter rate, $\Xi(E_I)$, during exposure of the ice to xenon beams of different E_I is proportional to the change in ice coverage as shown in Eq. (2):

$$-\frac{d\theta_{\mathrm{ice}}}{dt} = \eta\,\Xi(E_I). \tag{2}$$

Now, inserting Eq. (2) into Eq. (1) and rearranging to solve for the CID cross section gives

$$\sigma_{\mathrm{CID}}(E_I) = \frac{-\frac{d\theta_{\mathrm{ice}}}{dt}}{\Phi_{\mathrm{Xe}}\theta^0_{\mathrm{ice}}} = \frac{\eta\,\Xi(E_I)}{\Phi_{\mathrm{Xe}}\theta^0_{\mathrm{ice}}}. \tag{3}$$

It is important to note that the incident translational energy of the xenon atoms is a distribution, instead of a single value, meaning that the observed sputter rate is actually a convolution of the sputter rates of all of the energies in this distribution. A recent publication[30] demonstrated the importance of accounting for the width of the energy distribution

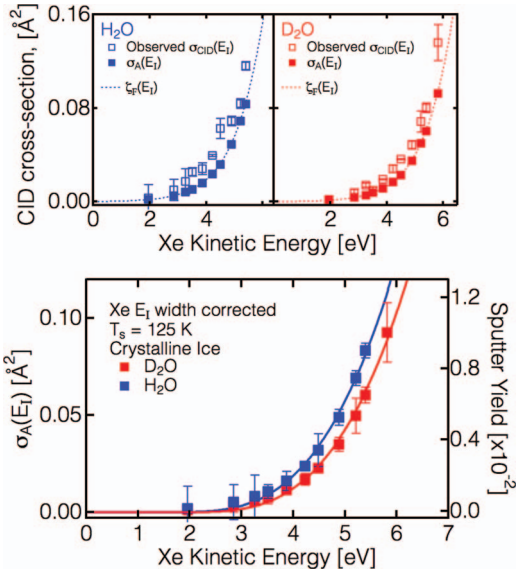

FIG. 3. Collision-induced desorption cross section and sputter yield, Y, of water from crystalline D_2O (red) and H_2O (blue) ice at 125 K on Au(111) for various xenon incident energies (E_I). The upper panels show the results of deconvolution of the actual cross section ($\sigma_A(E_I)$, solid symbols) from the experimental data ($\sigma_{CID}(E_I)$, open symbols). The dashed lines in the top panels are the $\zeta_F(E_I)$ ansatz. In the lower panel, the energy-width corrected data are plotted and the solid lines are hard-cube fits to the data as described in the text. The error bars represent the 2σ confidence interval from the average of at least three measurements for each data point.

when presenting results as a function of kinetic energy. To extract the actual functional dependence of the CID cross section on E_I, $\sigma_A(E_I)$, an ansatz is constructed, $\zeta_F(E_I)$, which fits the data well, and correctly expresses the incident energy dependence. Each collected data point, $\sigma_{CID}(E_I)$, is actually the ensemble-averaged CID cross section for an ensemble of xenon atoms with average energy, E_I, and incident energy distribution, $P(E_I)$. The integral of the product of $\zeta_F(E_I)$ and $P(E_I)$ yields $\sigma_{CID}(E_I)$, as given by Eq. (4):

$$\sigma_{CID}(E_I) = \int \zeta_F(E_I)\, P(E_I)\, dE_I. \tag{4}$$

To extract the actual values of the CID cross section at a given E_I, $\sigma_A(E_I)$, $\zeta_F(E_I)$ was approximated with a sigmoid function ($y(x) = c_1 + \frac{c_2}{1+\exp[(c_3-x)/c_4]}$, where the c_i's are the fitting parameters) for both H_2O and D_2O. The parameters of the ansatz were determined using a least-square fit, and then the sputtering cross sections, $\sigma_A(E_I)$, were calculated by inserting the average E_I's from the original dataset. The collected data points are shown in the upper panels of Figure 3 for H_2O (left) and D_2O (right), as well as $\zeta_F(E_I)$ and the corrected data points.

Finally, to compare the sputtering of water from thick ice films by neutral xenon atoms to other systems, the sputtering was also quantified by the sputter yield, Y, which is the number of water molecules desorbed for each incident xenon atom. The sputter yield with respect to the incident translational energy of xenon, $Y(E_I)$, is calculated from $\sigma_A(E_I)$ using Eq. (5):

$$Y(E_I) = \theta^0_{ice}\sigma_A(E_I). \tag{5}$$

The right axis of Figure 3 shows the sputter yield for D_2O and H_2O for various incident energies of xenon atoms. As seen in the figure, the yield increases with xenon E_I. The H_2O sputter yield is systematically greater than D_2O. This difference is likely due to the higher zero-point energy for hydrogen bonded H_2O in ice compared to D_2O.[37,38] The relatively low yield, at most 0.01 ejected D_2O or H_2O molecules per incident xenon atoms, is in agreement with the previous results for sputtering of thin (1–8 layers) films of ordered ice on Rh(111).[15] Translationally energized argon atoms, either 10 or 21 eV, sputtered about 0.001 water molecules per incident argon atom. The momentum of argon atoms with 10 or 21 eV translational energy is about the same as xenon with 3 or 6 eV of translational energy, and the sputter yields were nearly the same. Moreover, yields significantly less than unity were reported for low-energy ion sputtering of ice films.[39] As mentioned previously, ice films effectively absorb collisional energy because momentum transfer among the constituent molecules of the ice film is efficient. For sputtering of ices with high-energy ions, the insulating nature of the ice and the low mobility of charged particles in the ice cause a great enhancement of the sputtering yield, far greater than what would be expected if only accounting for the translational energy of the projectile.[12,26,40] When ions hit the surface, they alter the electronic structure of the ice, causing repulsive interactions and thus desorption.[10,24] These processes cannot occur with neutral projectiles unless the molecules are ionized by the collision. At the collision energies employed in these studies, sputtering caused by electronic effects does not occur because the lowest electronic states lie above the greatest xenon incident energies employed here.[41,42]

ASW forms during vapor deposition of water on cold substrates because when the water molecules stick to the surface, they do not have sufficient energy to find and adopt the energetically ordered, crystalline structure; they are thus kinetically trapped in the glassy, disordered amorphous phase. In a similar fashion, it is possible that the repeated, energetic collisions between xenon and the crystalline ice surface could push molecules out of the crystalline structure, and because there is not enough thermal energy at 125 K for them to snap back into the crystalline structure, xenon bombardment could result in the amorphization of the surface of crystalline ice. Equivalently, amorphous solid water is metastable with respect to crystalline ice at 125 K,[21,32] and perhaps the surface of amorphous ice would be crystallized by the collisions, for the collisional energy could drive the molecules over the barrier into the energetically favorable crystalline structure. Tantalizing as these outcomes may be, it seems that collisional energy does not give rise to significant changes in the surface morphology under the conditions explored herein. As shown in the spectra in Figure 2, during exposure of crystalline ice to translationally excited xenon atoms, the infrared absorption peak shape was not altered, and only the intensity changed. This implies that there was no change in the structure or binding of the water molecules in the ice due to collisions of translationally energetic xenon atoms with the ice surface. If crystalline ice were converted to amorphous ice, a change in the shape of the features, characteristic of amorphous solid water absorption, would be expected. Because of

these two observations, there is no evidence that bombardment caused any appreciable change in the morphology of the ice surface. Similarly, for xenon impinging on amorphous ice, there were no changes in the absorption feature suggestive of surface crystallization. Finally, there were no apparent differences in the sputtering yield from either amorphous or crystalline ices. After several hours of experiments, a small accumulation of H_2O was seen on D_2O ices; this was from absorption of background H_2O in the UHV chamber, and was virtually unavoidable. It is also reasonable to assume accumulation of H_2O on H_2O ice from the background was the same. During xenon exposure, the H_2O partial pressure in the UHV chamber was around 1×10^{-10} Torr, which corresponds to about 0.3 layers of H_2O deposited per hour. This deposition was sufficient to obscure the dangling O–D peak, but was significantly less than any sputtering rate or even thermal desorption; thus, the small amount of background accumulation on the ice surface had no effect on the measurement of the xenon sputtering process.

To better understand the dynamics of the sputtering process, we employ a hard-cube model to fit the data and extract the threshold energy for sputtering. Though certainly not theoretically rigorous, it would be interesting if such a straightforward model could at least qualitatively describe the sputtering process. Such a model was devised by Szulczewski and Levis[43] to model the desorption of small molecules from metal surfaces. In this collision model, a gas particle of a given mass and energy strikes a single surface molecule, thereby depositing a portion of its incident energy into the molecule. The collisional energy exchange is calculated with the Baule (hard-sphere or hard-cube) approximation[44] and determines the energy available to facilitate desorption. The empirical model to fit the data is given in Eq. (6) where A and N are fitting parameters, E_I is the collision energy, and E_{thrs} is the threshold energy for collision-induced desorption. The fit parameters A and N were optimized, and then held constant when fitting the sputtering curves for each isotopologue,

$$\sigma_{\text{CID}}(E_I) = A\frac{(E_I - E_{\text{thrs}})^N}{E_I}. \quad (6)$$

The solid lines in the lower panel of Figure 3 show the data fits from this model. The best data fits yielded values for the fitting parameter E_{thrs} of 1.74 eV for D_2O and 1.48 eV for H_2O.[45] The lower energy requirement to desorb an H_2O molecule than for a D_2O molecule is expected because of the difference in the zero-point energies of the two isotopologues in the condensed phase. The model is in good agreement with the data for larger cross sections (higher yield) but as evident in the figure, significantly underestimates the sputtering yield in the low-energy regime. The hard-cube model we employed provides a lower limit on the extent of energy exchange between the ice surface and the incident gas-phase xenon, and thus the threshold energy from this model establishes an upper limit for the amount of incident energy of the xenon required to causes sputtering. Within the single-collision context of this model, because of the mass-match between xenon atoms and the ice surface, only around half of the initial translational energy of the xenon may be transferred to the ice surface.[43] This implies that the experimental E_{thrs} is the amount of incident translational energy required, not the energy needed to desorb a water molecule. Because over half of E_I must remain with the Xe, in the context of this model, the actual energetic requirement to sputter water from ice is the product of the incident energy and the kinematic factor (0.46 for D_2O and 0.43 for H_2O) and thus the threshold energy for desorption is 0.81 and 0.64 eV for D_2O and H_2O, respectively. These values for E_{thrs} are near the enthalpy of sublimation and desorption barrier (between 0.515 to 0.536 eV) reported for a variety of different ice morphologies near 150 K.[45] It is also worth comparing the sputtering threshold energy to the cohesive strengths of water clusters of various sizes. The dissociation energy (the energy required to expel a single water molecule from the cluster) is 0.20 eV for the dimer and is 0.83 eV for the trimer. For clusters larger than the trimer, the dissociation energy monotonically decreases to the bulk water value of 0.25 eV per hydrogen bond.[45] The apparent sputtering threshold of 0.68 eV is near the dissociation energy for both the water tetramer and pentamer. These results suggest that the threshold energy from the model is plausible, given the energetic requirements to liberate a water molecule from ice. We further tested the validity of this model by measuring the energy of the scattered xenon and agreement was not found.

This model only accounts for energy exchange through a single impulsive collision, whereas the actual collisions are likely to be a more complicated series of events, beyond the scope of such a simple model. One other aspect we considered was the relationship between collision energy in the Laboratory and center-of-mass frames of reference. If the assumptions implicit in a hard-cube model were appropriate for this system, it would be important to describe the collision in terms of the center-of-mass collision energy. However, as we will explain further, sputtering of water from ice is likely the result of a multiple-collision process, rather than a single-collision process that is the basis of the hard-cube model. To better understand the dynamics of collision between translationally energetic xenon and ice surfaces, we measured the energy of the xenon scattered from the surface. Figure 4 shows the in-plane scattering intensity vs. final energy of 6.5 eV xenon at normal incidence scattered from a crystalline ice surface at a scattering angle of 45°. There are two scattering channels seen in the data: the fast channel has xenon atoms with translational energies of a few hundred meV, and a slower channel where the atoms have a Maxwell-Boltzmann energy distribution with a width characterized by the surface temperature, the trapping-desorption channel. The xenon atoms scattered through the trapping-desorption channel have lost any memory of their initial energy and have thermally equilibrated with the ice surface prior to desorption. Xenon atoms in the fast channel have not thermalized with the ice surface but still have lost most of their initial translational energy to the ice; an example is shown in Figure 4(a). The limitations of the hard-sphere model are evident in that it does not properly account for the energy loss of the colliding xenon. Energy exchange between the incident xenon atoms and the ice surface is much more extensive than simple momentum transfer between one atom and one surface molecule. It is worth comparing the dynamics of xenon scattering from ice to

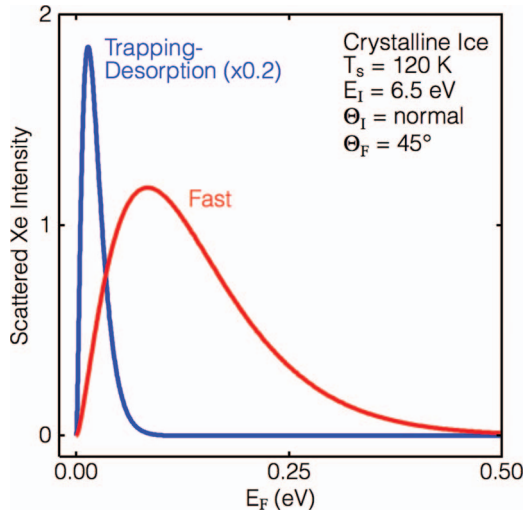

FIG. 4. Scattering data for in-plane scattering of xenon with $E_I = 6.5$ eV at normal incidence from crystalline D_2O ice of several hundred layers thickness on Rh(111) at 115 K, for a scattering angle of 45°. The red line in the plot is xenon scattered through the fast scattering, and the trapping-desorption channel is shown by the blue line. The trapping-desorption data is scaled by a factor of five to get the two plots on the same scale.

other systems where a heavy projectile impinges on a lighter surface. In the case of a light projectile (atom or molecule) hitting a heavy target, the incident species often scatters after a single collision. However, when the situation is reversed, and a heavy projectile strikes a light target, the scattering is more complicated. The incoming xenon atom crashes into the surface of the ice and drives the surface molecule into the underlying layer from which it recoils. The xenon atom is then pushed back into the vacuum by the elastic response of the surface as a whole. If the molecule still retains enough energy to overcome its bonding to the ice, it will desorb from the surface. This violent collision alters the hydrogen bond network of the ice, changing the binding among the surface water molecules, and can facilitate expulsion of a surface molecule. Another outcome of these energetic collisions is that the xenon can penetrate beneath the surface of the ice and become stably embedded within the solid. A publication by Gibson *et al.*[46] shows that xenon implants beneath the surface and becomes kinetically trapped. A second upcoming publication by them,[47] where experiments and theoretical simulations were combined, suggests desorption may also be the result of a cascade of collisions, where the initial collision imparts energy to some of the water molecules which undergo further collisions with other water molecules, and it is one of these that desorbs. This possibility was investigated by scattering xenon, krypton, and argon from GaAs(110) surfaces.[48] Although the xenon scattering was a multiple collision event, the dynamics could be described well by a binary collision between the projectile and a single surface atom.

CONCLUSIONS

Water molecules can be ejected from an ice surface by the collisions between energetic gas-phase xenon atoms and the ice surface. The results presented here show that there is a threshold for CID and that the sputter yield systematically increases with additional translational energy. The existence of the threshold energy is indicative of there being a single barrier to desorption. When the incident xenon translational energy is below the sputtering threshold energy, xenon collisions cannot desorb water, for the collision does not bring sufficient energy to surmount the desorption (or sublimation) barrier. Although ice efficiently dissipates collisional energy, sputtering still occurs. This implies that while energy exchange though the hydrogen bond network of the ice is rapid, it is not so fast as to totally prevent collision-induced desorption. In earlier CID studies of light adsorbates on heavy metal surfaces, sputtering was the result of hindered momentum transfer localizing energy in the comparatively weak surface-adsorbate bond, thus facilitating desorption. In contrast, in ice, momentum transfer is facile, and the xenon atoms may undergo more than one collision before being scattered back into the gas phase. After the momentum of a xenon atom has been reversed, it may also strike a water molecule with sufficient energy to eject it from the ice surface. In addition to the fundamental gas-surface collision dynamics issues discussed herein, we also note in closing that sputtering of solids with neutral species holds promise of becoming an insightful probe of surface composition including trace detection of adsorbed and absorbed species. It also holds promise as a gentle surface preparation method for soft materials due to the absence of charging effects arising from the use of charged projectiles or the subsequent ejection of ionic species.

ACKNOWLEDGMENTS

The authors gratefully acknowledge support from the Air Force Office of Scientific Research. Infrastructure support from the NSF Materials Research Science and Engineering Center at the University of Chicago, Grant No. NSF-DMR-0820054, further enabled this project.

[1]J. D. Beckerle, Q. Y. Yang, A. D. Johnson, and S. T. Ceyer, J. Chem. Phys. **86**, 7236 (1987).
[2]H. Gnaser, *Sputtering by Particle Bombardment* (Springer-Verlag, Berlin, 2007), Vol. 110, p. 231.
[3]B. J. Garrison and N. Winograd, Science **216**, 805 (1982).
[4]B. Y. Yu *et al.*, Anal. Chem. **80**, 3412 (2008).
[5]M. Gsell, P. Jakob, and D. Menzel, Science **280**, 717 (1998).
[6]U. Valbusa, C. Boragno, and F. B. de Mongeot, J. Phys.: Conden. Matter **14**, 8153 (2002).
[7]R. Gago, L. Vazquez, R. Cuerno, M. Varela, C. Ballesteros, and J. M. Albella, Appl. Phys. Lett. **78**, 3316 (2001).
[8]B. J. Bachman and M. J. Vasile, J. Vac. Sci. Technol. A **7**, 2709 (1989).
[9]K. J. Maynard, A. D. Johnson, S. P. Daley, and S. T. Ceyer, Faraday Discuss. **91**, 437 (1991).
[10]M. Asscher and Y. Zeiri, J. Phys. Chem. B **107**, 6903 (2003).
[11]A. D. Johnson, S. P. Daley, A. L. Utz, and S. T. Ceyer, Science **257**, 223 (1992).
[12]C. T. Reimann, J. W. Boring, R. E. Johnson, J. W. Garrett, K. R. Farmer, W. L. Brown, K. J. Marcantonio, and W. M. Augustyniak, Surf. Sci. **147**, 227 (1984).
[13]W. L. Brown, L. J. Lanzerotti, and R. E. Johnson, Science **218**, 525 (1982).
[14]W. L. Brown, L. J. Lanzerotti, J. M. Poate, and W. M. Augustyniak, Phys. Rev. Lett. **40**, 1027 (1978).
[15]K. D. Gibson, D. R. Killelea, and S. J. Sibener, J. Phys. Chem. C **113**, 13325 (2009).
[16]M. Inamura, T. Takaoka, and T. Komeda, Surf. Sci. **601**, 1072 (2007).
[17]J. Libuda and G. Scoles, J. Chem. Phys. **112**, 1522 (2000).
[18]J. Libuda and G. Scoles, J. Phys. Chem. B **103**, 9933 (1999).

[19]Y. Lilach, L. Romm, T. Livneh, and M. Asscher, J. Phys. Chem. B **105**, 2736 (2001).
[20]G. Szulczewski and R. J. Levis, J. Chem. Phys. **103**, 10238 (1995).
[21]R. J. Speedy, P. G. Debenedetti, R. S. Smith, C. Huang, and B. D. Kay, J. Chem. Phys. **105**, 240 (1996).
[22]J. D. Beckerle, A. D. Johnson, and S. T. Ceyer, J. Chem. Phys. **93**, 4047 (1990).
[23]J. D. Beckerle, A. D. Johnson, and S. T. Ceyer, Phys. Rev. Lett. **62**, 685 (1989).
[24]P. C. Sanfelix, A. Al-Halabi, G. R. Darling, S. Holloway, and G. J. Kroes, J. Am. Chem. Soc. **127**, 3944 (2005).
[25]A. Al-Halabi, P. C. Sanfelix, S. Holloway, G. J. Kroes, and G. R. Darling, Surf. Sci. **600**, 4247 (2006).
[26]R. Pedrys, F. Krok, P. Leskiewicz, J. Schou, U. Podschaske, and B. Cleff, Nucl. Instrum. Methods Phys. Res. B **164**, 861 (2000).
[27]R. A. Baragiola, R. A. Vidal, W. Svendsen, J. Schou, M. Shi, D. A. Bahr, and C. L. Atteberrry, Nucl. Instrum. Methods Phys. Res. B **209**, 294 (2003).
[28]A. Yabushita, T. Hama, M. Yokoyama, M. Kawasaki, S. Andersson, R. N. Dixon, M. N. R. Ashfold, and N. Watanabe, Astrophys. J. Lett. **699**, L80 (2009).
[29]S. Andersson and E. F. van Dishoeck, Astron. Astrophys. **491**, 907 (2008).
[30]K. D. Gibson, D. R. Killelea, H. Yuan, J. S. Becker, and S. J. Sibener, J. Chem. Phys. **134**, 034703 (2011).
[31]H. Yuan, D. R. Killelea, S. Tepavcevic, S. I. Kelber, and S. J. Sibener, J. Phys. Chem. A **115**, 3736 (2011).
[32]R. S. Smith, C. Huang, E. K. L. Wong, and B. D. Kay, Surf. Sci. **367**, L13 (1996).
[33]D. R. Killelea, V. L. Campbell, N. S. Shuman, and A. L. Utz, Science **319**, 790 (2008).
[34]P. A. Thiel and T. E. Madey, Surf. Sci. Rep. **7**, 211 (1987).
[35]B. D. Kay, K. R. Lykke, J. R. Creighton, and S. J. Ward, J. Chem. Phys. **91**, 5120 (1989).
[36]K. D. Gibson, M. Viste, and S. J. Sibener, J. Chem. Phys. **112**, 9582 (2000).
[37]C. G. Swain and R. F. W. Bader, Tetrahedron **10**, 182 (1960).
[38]J. D. Bernal and G. Tamm, Nature (London) **135**, 229 (1935).
[39]M. Fama, J. Shi, and R. A. Baragiola, Surf. Sci. **602**, 156 (2008).
[40]W. L. Brown, W. M. Augustyniak, K. J. Marcantonio, E. H. Simmons, J. W. Boring, R. E. Johnson, and C. T. Reimann, Nucl. Instrum. Methods Phys. Res. B **1**, 307 (1984).
[41]P. H. Hahn, W. G. Schmidt, K. Seino, M. Preuss, F. Bechstedt, and J. Bernholc, Phys. Rev. Lett. **94**, 4 (2005).
[42]D. M. Chipman, J. Chem. Phys. **122**, 10 (2005).
[43]G. Szulczewski and R. J. Levis, J. Chem. Phys. **98**, 5974 (1993).
[44]V. Celli, D. Himes, V. Bortolani, G. Santoro, J. P. Toennies, and G. Zhang, Surf. Sci. **242**, 518 (1991).
[45]P. Pratte, H. van den Bergh, and M. J. Rossi, J. Phys. Chem. A **110**, 3042 (2006).
[46]K. D. Gibson, D. R. Killelea, H. Yuan, J. S. Becker, and S. J. Sibener, Chem. Phys. Lett. **531**, 18–21 (2012).
[47]K. D. Gibson, D. R. Killelea, H. Yuan, J. S. Becker, S. Pratihar, P. Manikandan, W. L. Hase, and S. J. Sibener (unpublished).
[48]A. Amirav, M. J. Cardillo, P. L. Trevor, C. Lim, and J. C. Tully, J. Chem. Phys. **87**, 1796 (1987).